CHAPTER 3

RESULTS AND DISCUSSION

3.1 Electrode Response for Amino Acid in Batch Analysis

3.1.1 Effect of Buffer

The pH of supporting electrolyte was important because the reaction of the metal ions with the anionic form of the amino acids can be studied at pH's significantly beyond the pI of the amino acids(20). Therefore the pH of buffer systems, that chosen in this study must be high enough to give anionic form of amino acids. The selected buffers are phosphate buffer pH 7.0, carbornate buffer pH 10.2 and borate buffer pH 8.5.

The anodic voltammograms at a copper electrode in phosphate buffer solution and in phosphate buffer solution with cysteine concentration range 10^{-4} -10^{-5} M are presented in Figure 3.1 A. It can be seen that when the potential is change from -250 mV in the positive direction, the recorded curve resembles a D.C. voltammogram. The limiting current was not changed significantly up to applied potential of +250 mV but above +250 mV the current begun to decrease. Apparently the oxide film on the electrode surface were disrupted at very positive potentials. Addition of amino acid to the solution raised the limiting current reproducibly.

Voltammograms of a carbonate buffer solution are shown in Figure 3.1 C. Again the anodic current first increases

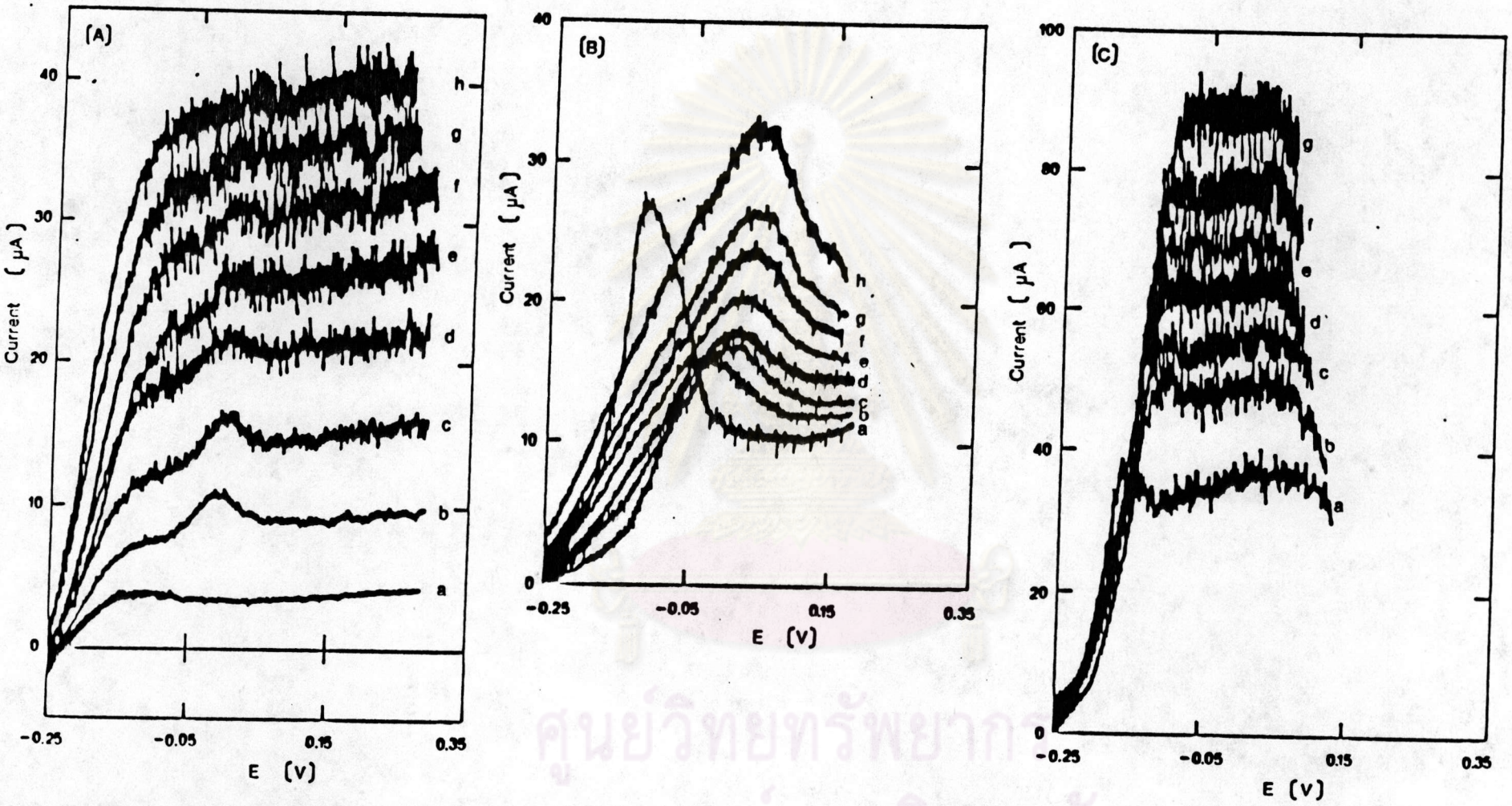

Figure 3.1 Voltammograms in (A) phosphate buffer pH 7.0, (B) borate buffer pH 8.5, and (C) carbonate buffer pH 10.2. Scan rate 2 mVs^{-1} ; stirred speed number 4, cysteine concentration : (a) 0.00 ; (b) 1.00×10^{-4} ; (c) 2.00×10^{-4} ; (d) 3.0×10^{-4} ; (e) 4.00×10^{-4} ; (f) 5.00×10^{-4} ; (g) 6.00×10^{-4} ; (h) 7.00×10^{-4} M.

exponentially with the potential until a limiting is reached. This limit background current is considerably higher than in phosphate buffer because the pH of the carbonate buffer is higher than that of the phosphate buffer, copper(II) ions clearly form much stronger complexes with carbonate ions than with phosphate ions.

Voltammograms of the amino acid measured in a borate buffer show maximum at about 0 mV (Figure 3.1B). These voltammograms are different from those obtained in phosphate buffer and carbonate buffer as they are peak-shaped wave instead of sigmoidal wave.

The cause of this different electrode behaviour must be sought in the structure of the oxide layers on the electrode surface; copper(II) ions formed by the electrode reaction must diffuse through the oxide (or hydroxide) layers and the permeability of these layers will therefore determine the electrode kinetics. In phosphate and carbonate buffer, the electrode kinetics is fast, while in borate buffer the electrode kinetics is slow as mentioned by Kok, et.al.(17).

The background currents and signal currents of 5.00×10^{-4} M cysteine were measured at the fixed potential of +150 mV, +150 mV and +50 mV in phosphate buffer, borate buffer and carbonate buffer, respectively. The results from Table 3.1 demonstrated that phosphate buffer was the best buffer since it provided the highest signal current to background current ratio (S/B) and the voltammograms give plateau at limiting current.

The effect of pH of the phosphate buffer solution on the limiting current was examined. The phosphate buffer pH 6.2, pH 7.0 and pH 8.2 were used in this study. The results obtained in Table 3.2

showed that S/B in the buffer pH 8.2 was little higher than that in the buffer pH 7.0, however the buffer capacity of the buffer pH 7.0 was the highest. When the pH is high, it increases participation of the equilibria involving hydroxyl ions. Therefore, phosphate buffer pH 7.0 was selected for all subsequent studies.

Table 3.1 Anodic limiting current at copper electrode in various supporting electrolytes

supporting electrolyte	background current, μA	signal current, μA	S/B
phosphate buffer	3.13	14.39	4.59
borate buffer	8.50	6.00	0.92
carbonate buffer	18.00	12.17	0.68

Table 3.2 Effect of pH on background current and signal current

pH of phosphate buffer	buffer capacity	background current, μA	signal current, μA	S/B
6.2	0.005	14.90	1.98	0.13
7.0	0.02	3.38	3.80	1.12
8.2	0.01	2.80	3.44	1.23

Voltammogram of phosphate buffer pH 7.0 in Figure 3.1 shows that the limiting current was steady in the potential range 100-200 mV. Thus, the potential at +150 mV was employed for amino acid determination at fixed operating potential (amperometry).

3.1.2 Effect of Stirred Speed

The effect of stirred speed was examined in phosphate buffer pH 7.0 and 5.00×10^{-4} M cysteine in phosphate buffer pH 7.0. The obtained results were shown in Table 3.3 and Figure 3.2 which was the plot of the signal current to the background current ratio (S/B) against stirred speed number. The curve showed that the S/B increased with the stirred speed up to number 5 and there was no significant increase when stirred speed higher than number 5 was employed. At stirred speed up to number 5, dependence on stirred speed can be attributed to increase convective mass transport at the electrode. Further increase in stirred speed gives little increase in the analyte signal. This can be attributed to the rate-limiting step for electron transfer at the electrode, which is independent of mass

Table 3.3 Effect of stirred speed on limiting current and background current

stirred speed number	background current,μA	signal current,μA	S/B
0	1.00	2.53	2.53
1	2.01	6.64	3.30
2	2.57	9.36	3.64
3	3.00	11.95	3.98
4	3.22	14.41	4.48
5	3.20	15.30	4.78
6	3.20	15.55	4.86
7	3.20	15.80	4.94

transport, and complexation reaction between copper(II) ions and amino acids. It was found that the stirred speed number 4 was the most suitable although the stirred speed higher than number 4 will give higher S/B but it will also lead to the irregular stirring by the magnetic bar.

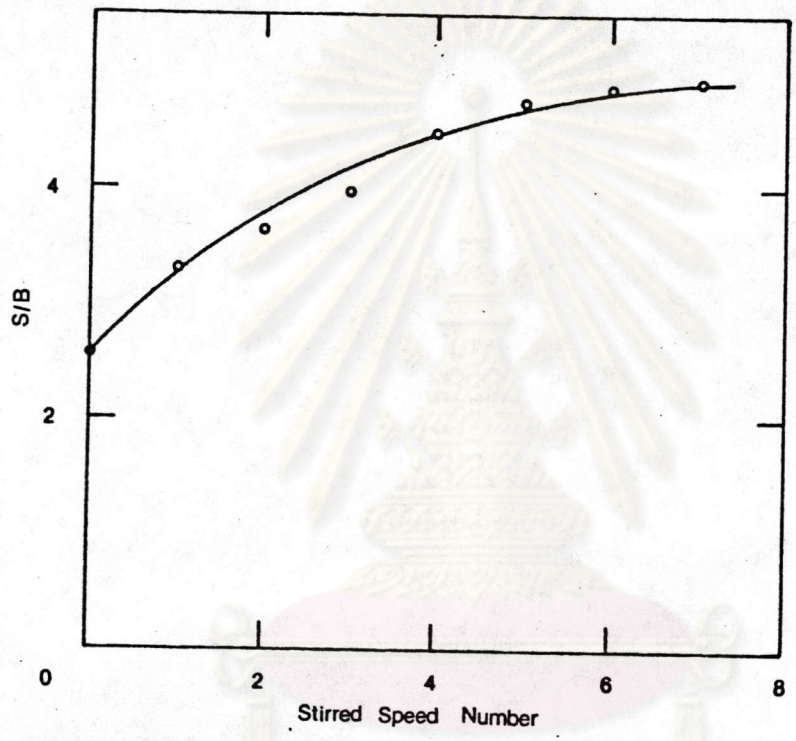

Figure 3.2 Effect of stirred speed on S/B

3.1.3 Study of Copper(II)-Amino Acid Ratio in Complex

The copper(II)-cysteine ratio in the complex was examined by the anodic limiting current method described in 2.3.4. The anodic current, measured at +150 mV, decreased when copper(II) ions were added to the phosphate buffer solution. At the copper concentration 5.17×10^{-5} M where precipitation begun, the anodic current

was nearly zero. Apparently chemical dissolution of the copper(II) film, the cause of the anodic current, was no longer possible. Afterwards, the phosphate buffer solution with 2.00×10^{-4} M cysteine was examined instead of the phosphate solution. The anodic current decreased when copper(II) ions were added to this solution (Figure 3.3). At the copper concentration 14.54×10^{-5} M where precipitation begun, the anodic current was nearly zero. Thus the concentration of copper(II) ions that used to form complex with 2.00×10^{-4} M cysteine was 9.37×10^{-5} M. This means that formation of the 1:2 copper(II)-cysteine complex is predominant in the bulk solution.

The copper(II)-cysteine ratio in the complex was also determined by the cathodic limiting current method described in 2.3.4. The cathodic limiting current increased with the concentration of copper(II) ions added until the precipitation was observed and after that the current would not increase further (Figure 3.3). The copper concentration required to give rise to the precipitation in the phosphate buffer solution and in the phosphate buffer solution with 2.00×10^{-4} M cysteine were 4.85×10^{-5} M and 14.32×10^{-5} M, respectively. Therefore the concentration of copper(II) ion that used to form complex with 2.00×10^{-4} M cysteine was 9.37×10^{-5} M. This means that formation of the 1:2 copper(II)-cysteine complex was obtained in agreement with that found by the anodic limiting current method.

Similar experiments were done with glycine and threonine, and the results were shown respectively in Figure 3.6-3.7. The effect on the anodic current and the cathodic current of these solutions when adding the copper(II) ions, was similar to that of

cysteine solution.

For glycine, at +150 mV the copper concentration required to give rise to constant current in the buffer solution and in the buffer solution with 2.00×10^{-4} M glycine were 3.40×10^{-5} M and 12.50×10^{-5} M, respectively. Thus 9.10×10^{-5} M copper(II) ions would form complex with 2.00×10^{-4} M glycine and the ratio was 1:2. At -250 mV the copper concentration required to give rise to constant current in the buffer solution and in the buffer solution with 2.00×10^{-4} M glycine were 4.95×10^{-5} M and 14.56×10^{-5} M, respectively. Therefore, 9.51×10^{-5} M copper(II) ions would form complex with 2.00×10^{-4} M glycine and the ratio was 1:2.

For threonine at +150 mV the copper concentration required to give rise to constant current in the buffer solution and in the buffer solution with 2.00×10^{-4} M threonine were 3.45×10^{-5} M and 14.41×10^{-5} M, respectively. Thus, 10.96×10^{-5} M copper(II) ions would form complex with 2.00×10^{-4} M threonine and the ratio was 1:2. At -250 mV the copper concentration required to give rise to constant current in the buffer solution and buffer solution with 2.00×10^{-4} M threonine were 4.95×10^{-5} M and 15.32×10^{-5} M , respectively. Therefore, 10.37×10^{-5} M copper(II) ions would form complex with 2.00×10^{-4} M threonine and the ratio was 1:2.

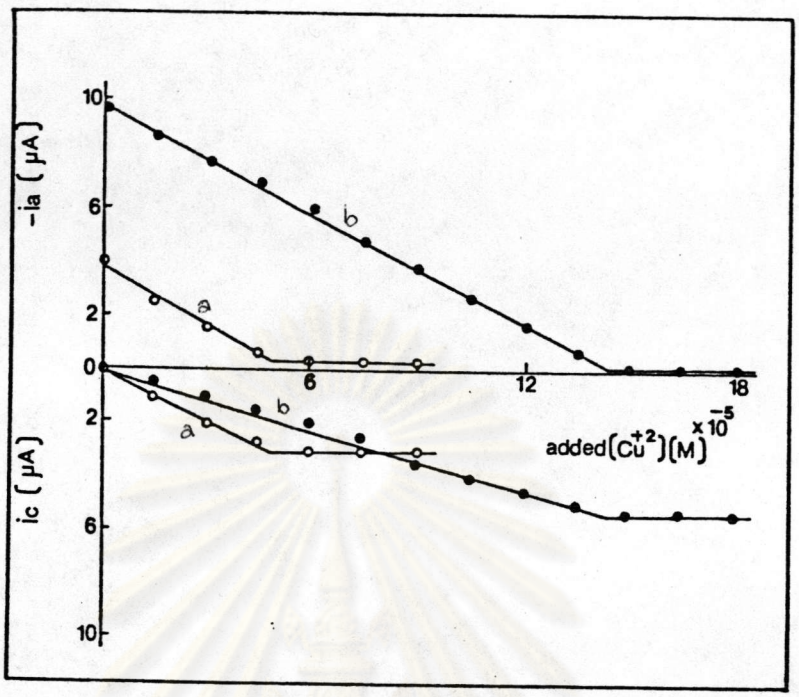

Figure 3.3 Anodic and cathodic current. Cysteine concentration:
(a) 0.00 ; (b) 2.00×10^{-4} M

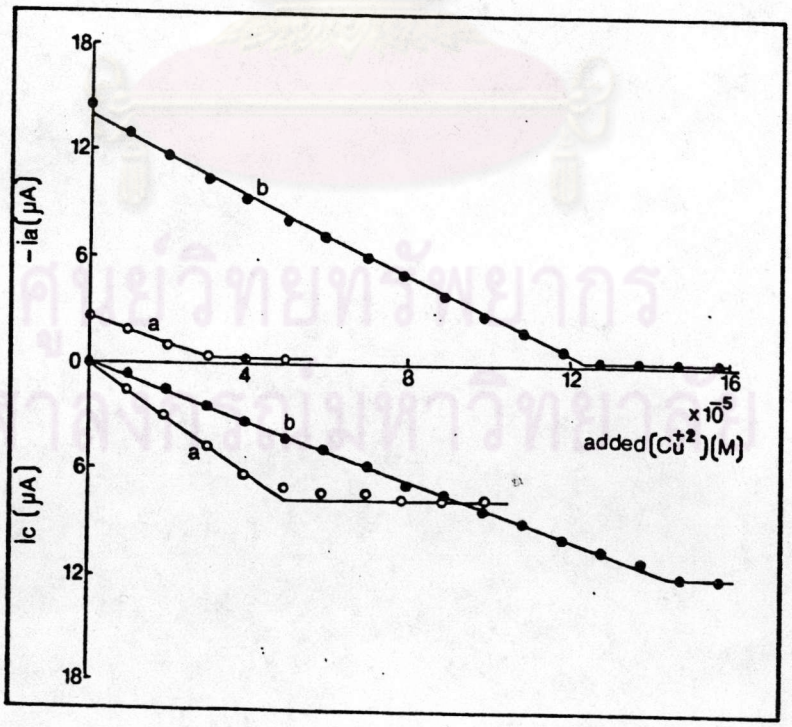

Figure 3.4 Anodic and cathodic current. Glycine concentration:
(a) 0.00 ; (b) 2.00×10^{-4} M

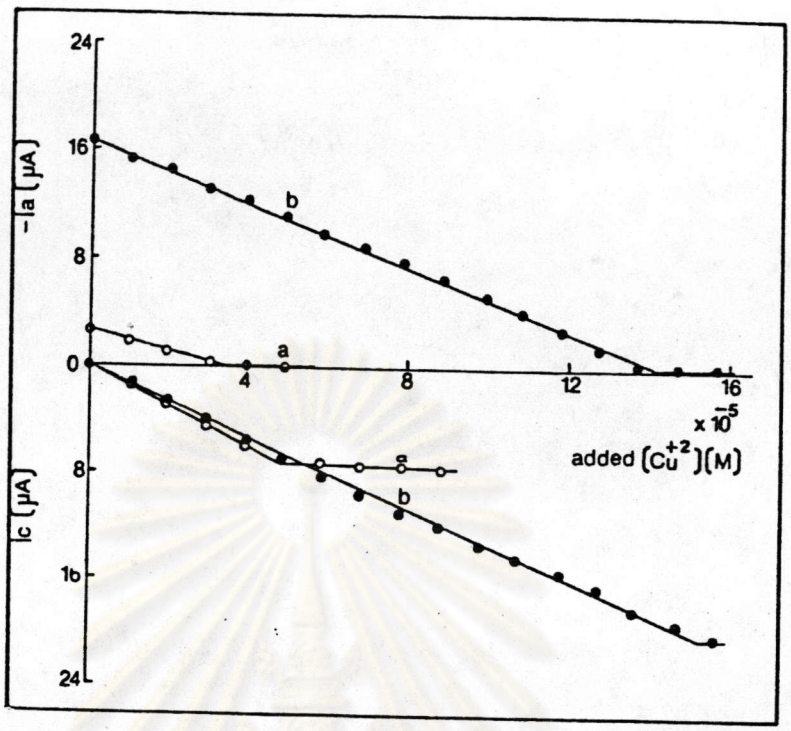

Figure 3.5 Anodic and cathodic current. Threonine concentration:
(a) 0.00 ; (b) 2.00×10^{-4} M

The summary of these results from anodic and cathodic current methods are shown in Table 3.4-3.5, respectively. The results show that the copper(II)-amino acid ratio is approximately 1:2. Since the 1:2 complex was formed, the stability constant will be of the order of 10^{15} (20). Under these conditions, the forward reaction rate can be very high, where as the reverse reaction will obviously be slow, so that complexation may be regarded as an instantaneous, irreversible reaction. From this reason, the detection method, using dissolution of copper(II) ions from the copper electrode to form complex with amino acids,can be employed for the amino acid analyses.

Table 3.4 Determination of copper(II)-amino acid complex ratio by anodic limiting current method

amino acid	$[Cu(II)]_a$ ($\times 10^{-5}$ M)	$[Cu(II)]_b$ ($\times 10^{-5}$ M)	$[Cu(II)]_b - [Cu(II)]_a$ ($\times 10^{-5}$ M)	Ratio
cysteine	5.17	14.54	9.37	1:2.23
glycine	3.40	12.50	9.10	1:2.20
threonine	3.45	14.41	10.96	1:1.83

$[Cu(II)]_a$ = the concentration of copper(II) that required to give the beginning of constant current in the phosphate buffer

$[Cu(II)]_b$ = the concentration of copper(II) that required to give the beginning of constant current in the phosphate buffer with 2.00×10^{-4} M amino acid

$[Cu(II)]_b - [Cu(II)]_a$ = the concentration of copper(II) ion that required to form complex thoroughly with 2.00×10^{-4} M amino acid

Table 3.5 Determination of copper(II)-amino acid complex ratio by cathodic limiting current method

amino acid	$[Cu(II)]_a$ ($\times 10^{-5}$ M)	$[Cu(II)]_b$ ($\times 10^{-5}$ M)	$[Cu(II)]_b - [Cu(II)]_a$ ($\times 10^{-5}$ M)	ratio
cysteine	4.85	14.22	9.37	1:2.13
glycine	4.95	14.56	9.61	1:2.08
threonine	4.95	15.32	10.37	1:1.93

$[Cu(II)]_a$, $[Cu(II)]_b$ and $[cu(II)]_b - [Cu(II)]_a$ are the same as those in Table 3.4

3.1.4 Sensitivity and Linear Range

The simultaneous analysis of cysteine, glycine and threonine in phosphate buffer pH 7.0 were investigated. Effect of these amino acids concentrations on the signal current and calibration curves are illustrated in Table 3.6-3.8 and Figure 3.6-3.8 , respectively. The results show that the signal current was proportional to the amino acid concentration. The calibration plot is linear in a range of 2.49×10^{-5} - 5.21×10^{-4} M cysteine, 2.49×10^{-5} - 6.76×10^{-4} M glycine and 2.49×10^{-5} -5.44×10^{-4} M threonine. The sensitivity, as the slope of these calibration plots, are 66.67 mAM^{-1} cysteine, 50.68 mAM^{-1} glycine and 64.10 mAM^{-1} threonine with the same correlation coefficient of 0.999. The summary of these results is shown in Table 3.9.

Table 3.6 Effect of cysteine concentration on the signal current (in phosphate buffer pH 7.0 at the fixed potential of +150 mV)

[cysteine] ($\times10^{-5}$ M)	signal current (μA)
2.49	1.65
4.98	3.65
9.90	7.10
14.80	10.55
19.60	14.05
24.40	16.70
29.10	19.75
33.80	22.90
38.50	25.85
43.10	29.05
47.60	32.10
52.10	35.00

Table 3.7 Effect of glycine concentration on the signal current (in phosphate buffer pH 7.0 at the fixed potential of +150 mV)

[glycine] $(x10^{-5}$ M)	signal current μA
2.49	1.20
7.44	3.80
12.40	7.40
17.20	9.30
22.00	11.80
26.80	14.80
31.50	17.30
36.10	19.55
40.80	21.55
45.40	23.55
49.90	26.05
54.40	28.03
58.80	30.30
63.20	32.55
67.60	34.30

Table 3.8 Effect of threonine concentration on the signal current (in phosphate buffer pH 7.0 at the fixed potential of +150 mV)

[threonine] $(x10^{-5}$ M)	signal current μA
2.49	1.15
7.44	3.75
12.40	6.65
17.20	10.15
22.00	13.35
26.80	16.50
31.50	19.50
36.10	22.90
40.80	25.65
45.00	28.25
49.90	31.00
54.40	33.75

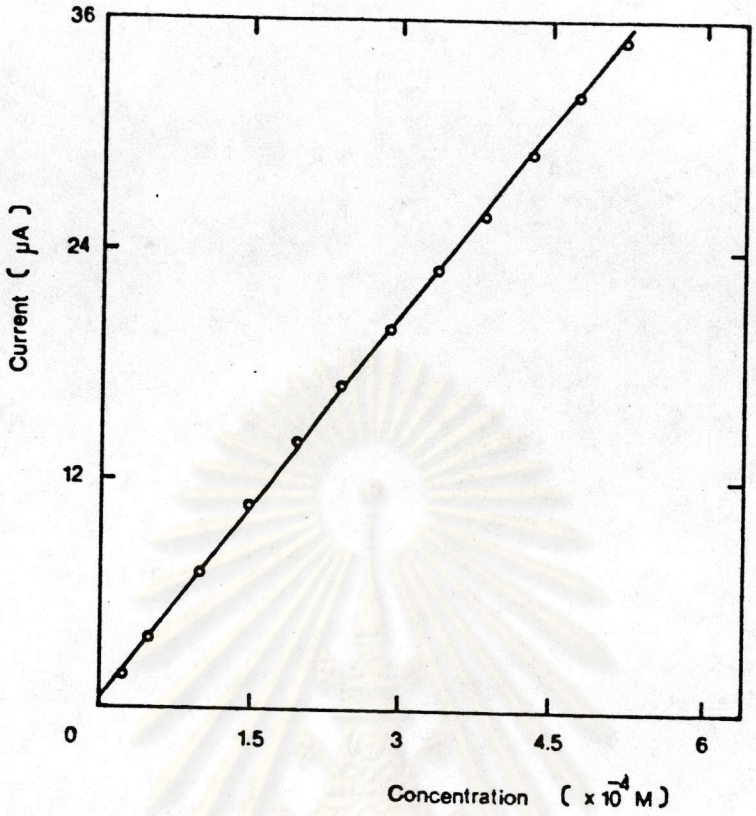

Figure 3.6. Calibration curve of cysteine in phosphate buffer pH 7.0

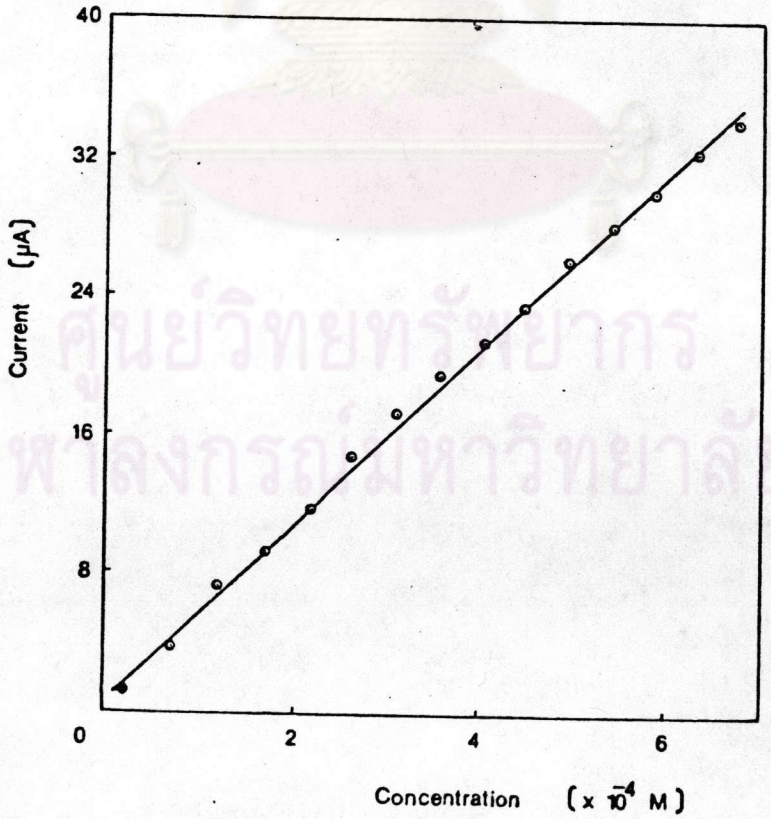

Figure 3.7 Calibration curve of glycine in phosphate pH 7.0

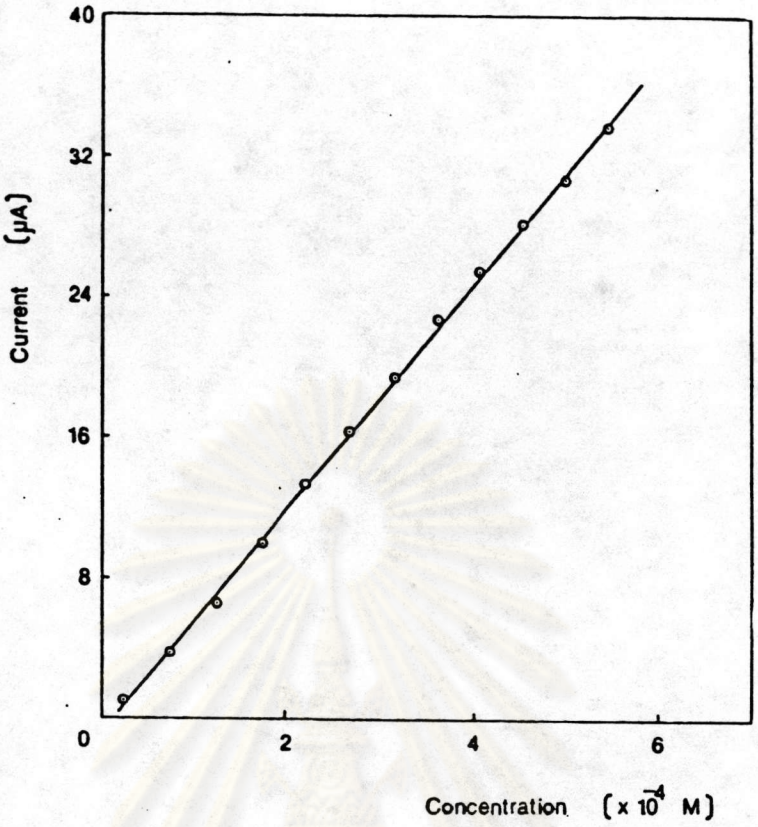

Figure 3.8 Calibration curve of threonine in phosphate buffer pH 7.0

Table 3.9 Electrode characteristics in batch analysis with amperometric detection

amino acid	sensitivity mAM^{-1}	linear range M	detection limit M
cysteine	66.67	2.49×10^{-5} -5.21×10^{-4}	5.00×10^{-8}
glycine	50.68	2.49×10^{-5} -6.76×10^{-4}	5.00×10^{-7}
threonine	64.10	2.49×10^{-5} -5.44×10^{-4}	8.00×10^{-7}

3.1.5 Reproducibility and Detection Limit

The detection limit for amino acid sample prepared in phosphate buffer pH 7.0 were determined by measuring the limiting current 10 replicates of 1.00×10^{-5} M ; calculated as 3 SD , the values obtained were 5.00×10^{-8} , 5.00×10^{-7} and 8.00×10^{-7} M for cysteine, glycine

and threonine, respectively (Table 3.9).

Reproducibility , as relative standard deviation , obtained for 10 replicates of the same sample were 0.67% for background current (phosphate buffer pH 7.0) , 1.05% for 1.00×10^{-4} M cysteine , 1.20% for 1.00×10^{-4} M glycine and 1.22% for 1.00×10^{-4} M threonine as shown in Table 3.10.

Table 3.10 Reproducibility of limiting current

limiting current of solution	% RSD
phosphate buffer	0.87
1.00×10^{-4} M cysteine	1.05
1.00×10^{-4} M glycine	1.20
1.00×10^{-4} M threonine	1.22

3.2 Electrode Response for Amino Acids in FIA

In the previous sections, it was shown that the current flowing through an anodized copper electrode in phosphate buffer solution increased linearly with increasing concentration of amino acids in the solution. In this study, the detection method used in batch system was applied to a flow-through cell with a copper electrode as an amperometric detector in FIA. The examinations were including effect of flow rate and residence time on peak current, effect of sampling rate on reproducibility and carryover, sensitivity, linear range and detection limit.

3.2.1 Effect of Flow Rate

In FIA, the response of the detector in terms of the residence time for each bolus at the detector was improved by increasing the flow rate (43). The improved response was observed by previous workers (95), and was due to two factors : (1) the increased mass transport from the flowing solution to the electrode surface, and (2) a reduction in the thickness of the diffusion layer.

The effect of flow rate on background current and peak current were examined by injecting 10 replicates of 0.01 M glycine solution to the flow stream of phosphate buffer pH 7.0. The results in Table 3.11 show that the background current increased with increasing flow rate in agreement with that found by other detection methods(95). However, the peak current decreased when flow rate increased. This is contradictory to that normally observed when the other detection methods were used in FIA. The reason for this phenomenon is that this detection technique is indirect method and the peak current is dependent on the concentration of copper(II) ion that dissolved from the copper electrode to form complex with amino acid. Thus, this electrode reaction was limited by the rate of complexation. The improved sensitivity can be attributed to the increased time period during the amino acid sample contacted with the electrode by decreasing flow rate.

The effect of flow rate on the reproducibility of the response at the copper electrode was also shown in Table 3.11. It was found that the reproducibility decreased with increasing flow rate owing to various factors including the irregular pumping of carrier

stream at high flow rate and the lower precision in the residence time when the manual injection technique was employed which would result in low reproducibility of dispersion zone at high flow rate.

Table 3.11 Effect of flow rate on background current, peak current and reproducibility for 10.0 µL injection of 0.01 M glycine into phosphate carrier stream at pH 7.0.

flow rate $mL\ min^{-1}$	background current, µA	peak current µA	S/B	% RSD
1	0.30	1.42	4.73	0.84
2	0.34	1.41	4.15	1.12
3	0.41	1.17	2.85	1.24
4	0.43	0.88	2.05	1.67
5	0.45	0.66	1.47	2.70

The effect of flow rate on sample peak widths was also examined by injecting 10.0 µL of 0.01 M amino acid (such as glycine, threonine and cysteine) and recorded the response with fast chart speed, as shown in Figure 3.9. The results from Figure 3.9 are summarized in Table 3.12 showing the peak widths for baseline resolution at various flow rates, together with the calculated change in sampling rate. The peak widths were found to be inversely related to the flow rate but sampling rate were found to be directly related to the flow rate.

From Table 3.11 and Table 3.12, the flow rate of 2 $mL\ min^{-1}$ was found to be the most suitable although the flow rate of 1 $mL\ min^{-1}$ gave little higher peak current to background ratio and little higher

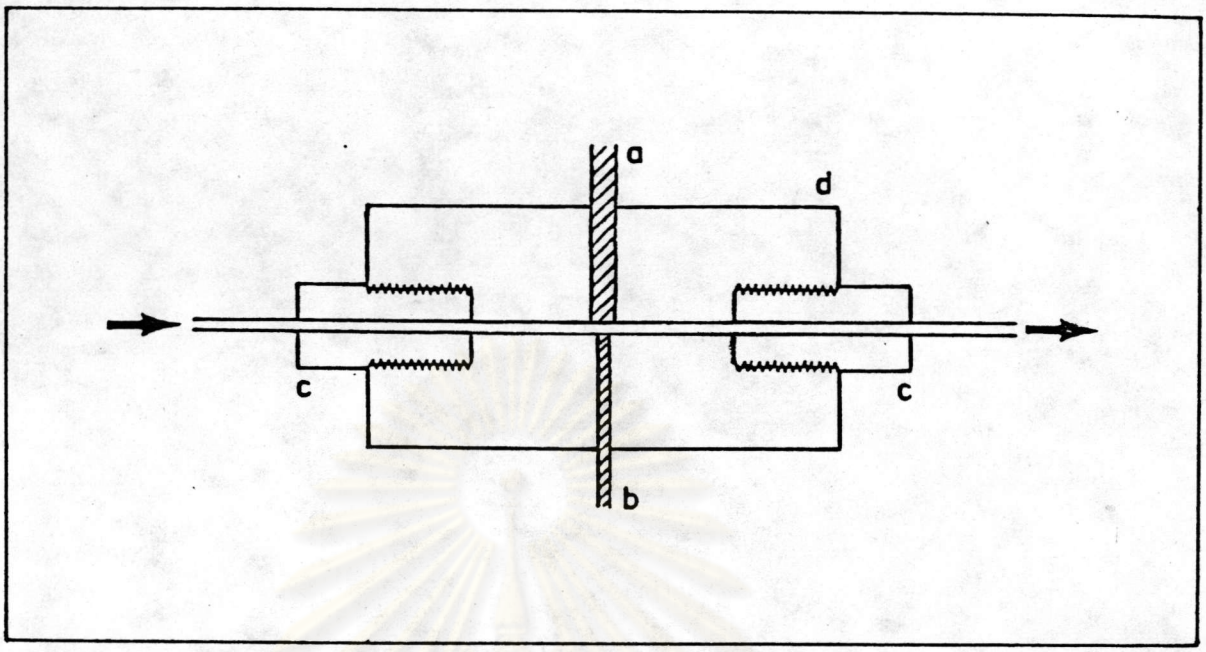

Figure 2.4 Flow cell constructed of high density polyethylene: (a) copper electrode; (b) platinum auxiliary electrode; (c) connectors (0.5 mm i.d.); (d) cylindrical body (1.0 mm i.d., 2.5 cm length, 1.2 cm diameter).

2.1.4 Instrumentation for HPLC

A Pye Unicam model PU 4010 pump was used. Sample injection was performed with a Reodyne 7125 equipped with a 20 µL sample loop. Separation of amino acids was on a Spherisorb ODS column (25 cm x 4.6 mm, particle size 5 µm), protected by a guard column. Detector was the same flow through cell as FIA.

2.1.5 Other Instrumentation

2.1.5.1 Hamilton micro-syringes (10,25 µL) were used for the injection of sample solution into the carrier steam for FIA and HPLC.

2.1.5.2 Finnpipette (50,250 µL) were used for the injection of sample solution into the buffer solution in batch system.

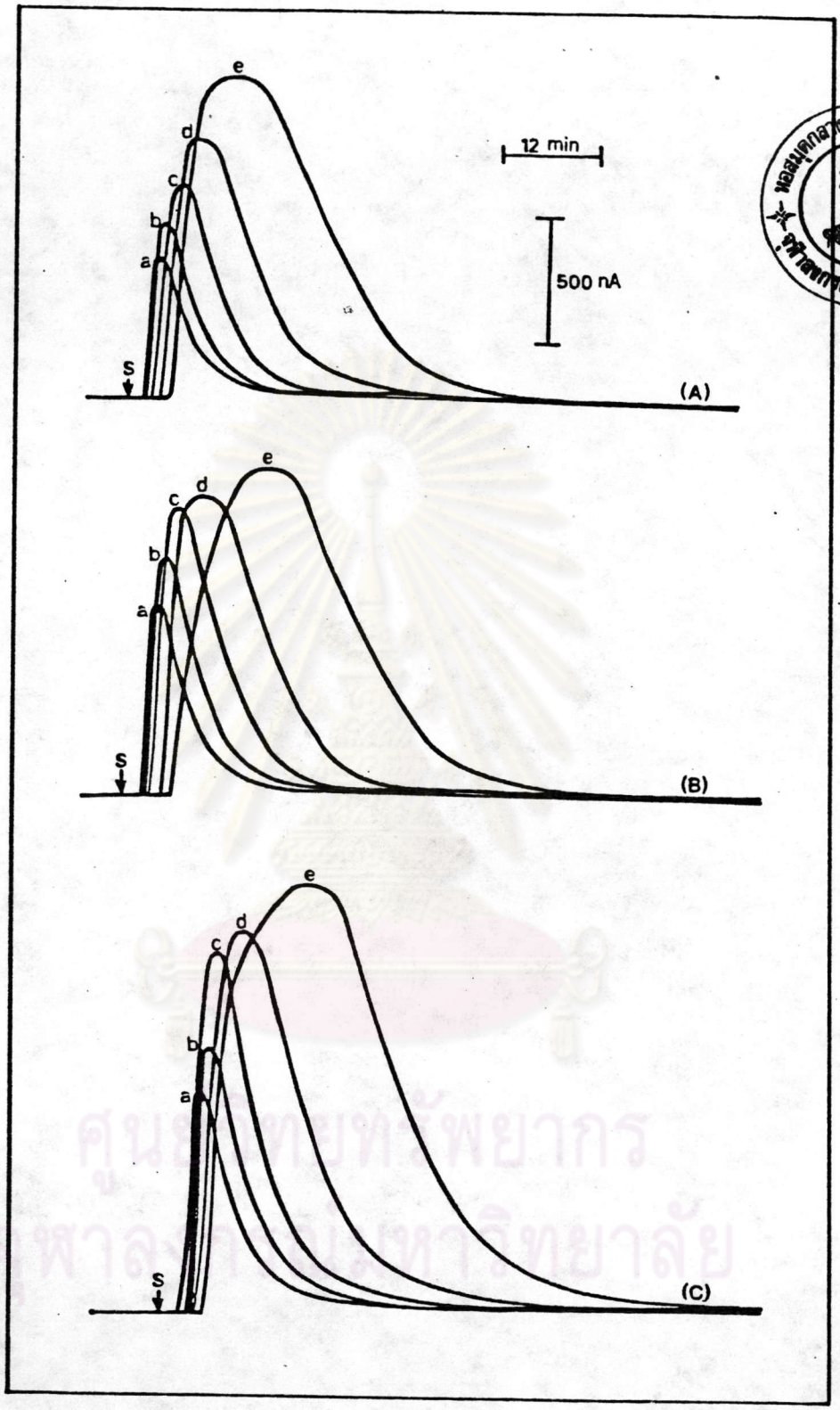

Figure 3.9 Effect of flow rate on sample peak width 10.0 µL injection and the following rates : (a) 5, (b) 4, (c) 3, (d) 2, (e) 1 mL min^{-1}, for 0.01 M amino acids: (A) glycine, (B) threonine, (C) cysteine

reproduciblity(low % RSD) than the fow rate of 2 mL min^{-1}, however, the calculated sampling rate at the flow rate of 2 mL min^{-1} was higher than that at the flow rate of 1 mL min^{-1} by 18 samples h^{-1} (for glycine)

Table 3.12 Effect of flow rate on sample peak width for 10.0 µL injection of 0.01 M amino acids into phosphate carrier stream at pH 7.0.

amino acid	flow rate, mL min^{-1}	peak width, s	calculation sampling rate, h^{-1}
glycine	1	42.9	84
	2	35.4	102
	3	24.0	150
	4	19.1	189
	5	16.5	218
threonine	1	51.6	70
	2	34.8	104
	3	27.6	130
	4	22.2	162
	5	21.8	165
cysteine	1	60.9	59
	2	49.9	72
	3	38.9	93
	4	33.3	108
	5	27.9	129

3.2.2 Effect of Residence Time

The effect of residence time was investigated by injecting 10.0 µL of 0.01 M glycine to the carrier stream at various tube length between injection port and flow-through electrochemical cell. The results obtained in Table 3.13 show that the peak current was inversely related to the residence time. Peak current was declined by the increase in dispersion which was due to the increasing of residence time. However, too short residence time produces turbulent

flow in the carrier stream which sample solution is injected, this will lead to the decrease in reproducibility of dispersion. Therefore the residence time at the tube length of 10.0 cm was adopted to use in the following studies.

Table 3.13 Effect of residence time in term of tube length on background current and peak current at the flow rate of 2 $mL\ min^{-1}$

tube length cm	background current, μA	peak current μA	S/B	% RSD
5.0	0.34	1.41	4.14	1.12
10.0	0.31	0.97	3.13	0.99
25.0	0.33	0.75	2.27	2.49
50.0	0.35	0.68	1.70	3.22

3.2.3 Effect of Sampling Rate on Reproducibility and Carryover

Sample interaction (carryover) leading to inaccurate results, is a problem in FIA. Carryover can be eliminated from FIA by employing a sufficient wash time between samples to allow the dispersed tail to approach the baseline closely. A longer time is usually required to flush through the sample in order to give the signal to reach the baseline. This effect of flush time therefore remained as a major factor limiting sampling rates in FIA.

Figure 3.10-3.11 demonstrate the effect of different sampling rates in the range of 80-144 samples h^{-1} on reproducibility of 10 replicate determinations and on carryover at the flow rate of

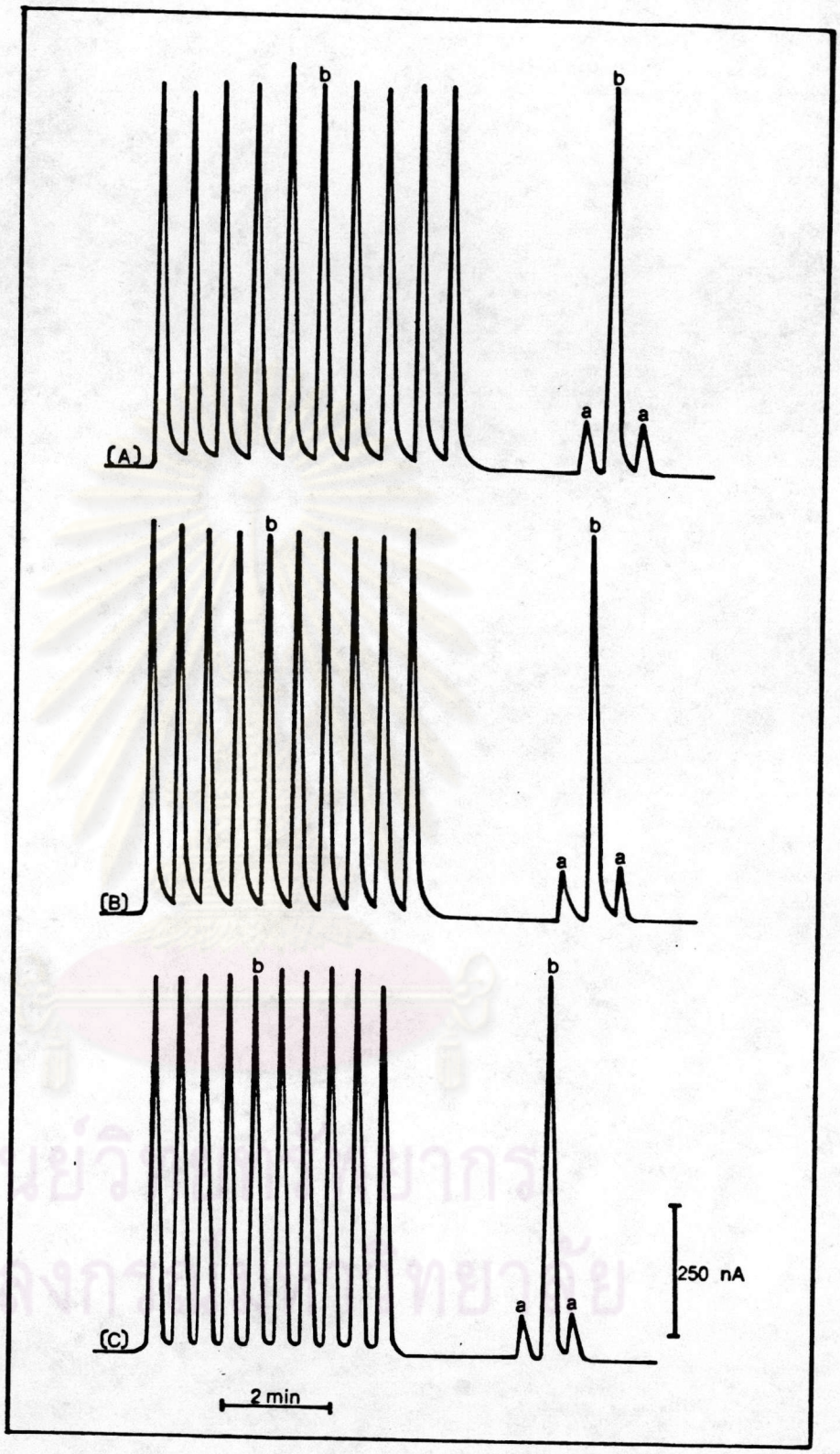

Figure 3.10 Effect of sampling rate on reproducibility and carryover at the flow rate of 2 mL min^{-1} : (A) 80, (B) 90, (C) 103 samples h^{-1} , for glycine concentrations: (a) 1.00×10^{-3} , (b) 6.00×10^{-3} M.

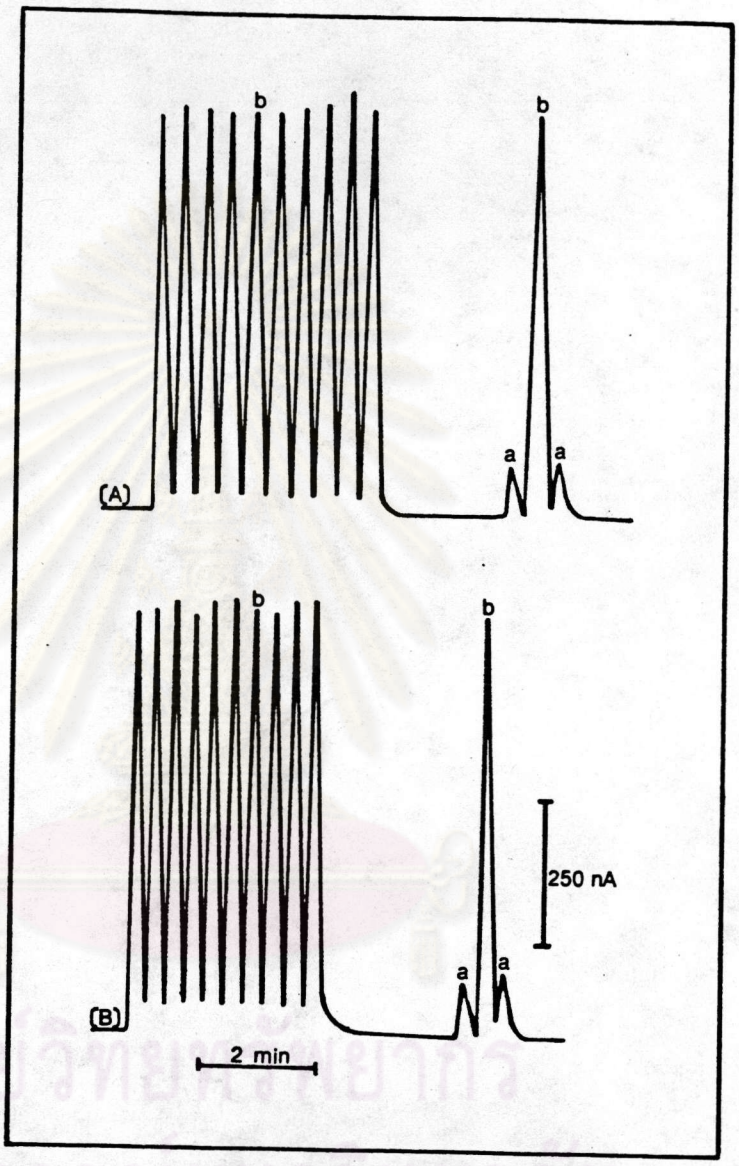

Figure 3.11 Effect of sampling rate on reproducibility and carryover at the fixed flow rate of 2 mL min^{-1} : (A) 120, (B) 144 samples h^{-1} , for glycine concentrations: (a) 1.00x10^{-3} , (b) 6.00x10^{-3} M.

2 mL min^{-1}. The calculations of these values were summarized in Table 3.14. It was shown that there was no carryover at sampling rate 80 samples h^{-1}, however the carryover increased with the increased in sampling rate. The reproducibility was in the range of 1.2-1.4%

Table 3.14 Effect of sampling rate on reproducibility and carryover.

Sampling rate samples h^{-1}	% RSD	% CO
80	1.45	0.00
90	1.14	1.33
103	1.26	1.37
120	1.43	2.13
144	1.21	2.70

3.2.4 Sensitivity, Linear Range and Detection Limit.

Injections of 10.0 µL of amino acid solutions (such as glycine, threonine and cysteine) gave sharp peaks, with heights in linear relationship to the amino acid concentrations as shown in Figure 3.12. Effect of glycine, threonine and cysteine concentrations on peak current in FIA and the calibration plots are shown respectively in Table 3.15-3.17 and Figure 3.13-3.15. The calibration plot is linear in the range of 5.00×10^{-4} - 1.00×10^{-1} M glycine, 5.00×10^{-4} - 1.00×10^{-1} M threonine and 5.00×10^{-5} - 6.00×10^{-3} M cysteine. The linear working range from calibration plots of amino acids were wide except cysteine which could not be determined at high concentration. Cysteine caused poisoning effects at the copper electrode and baseline

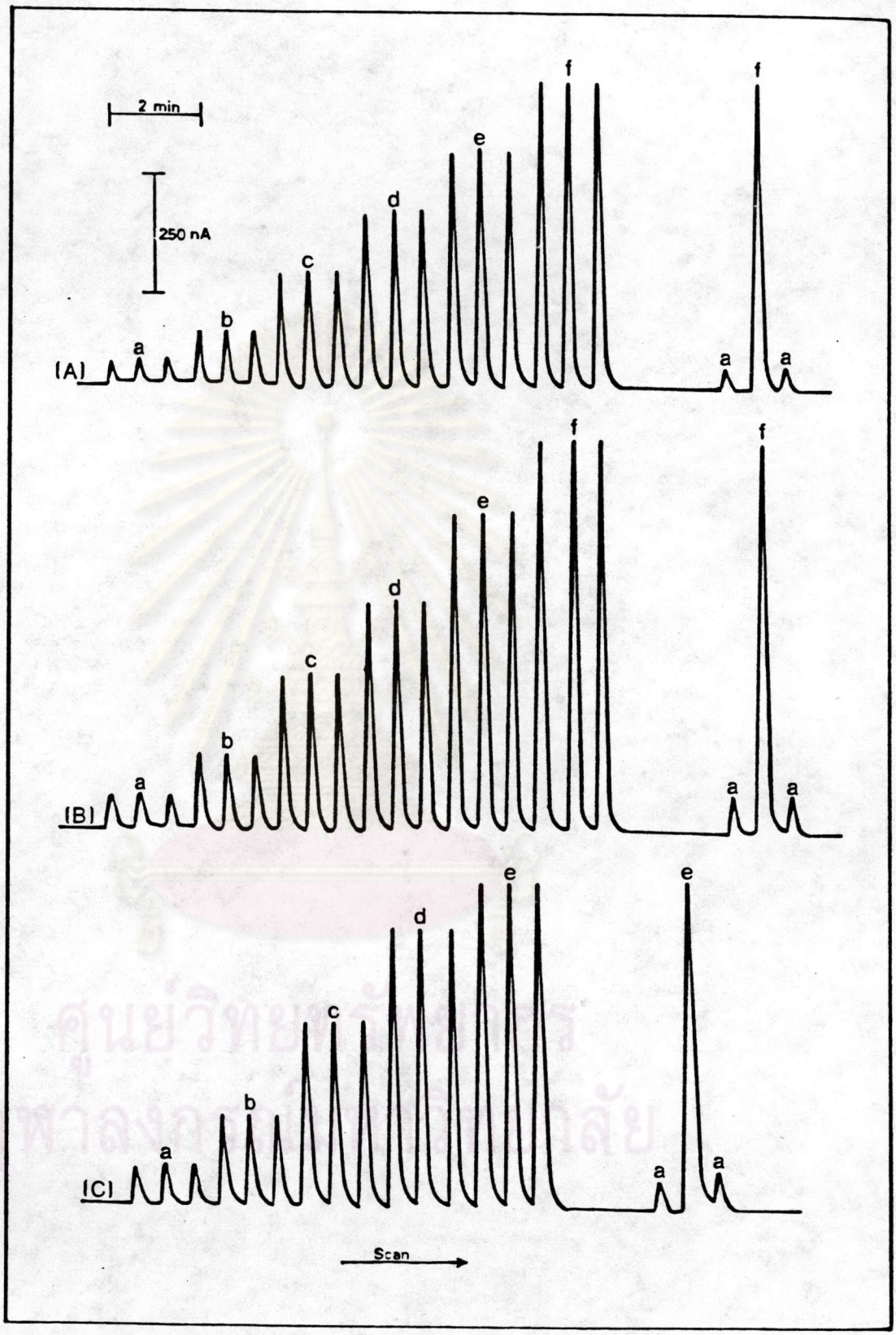

Figure 3.12 Effect of amino acid concentration on sample peak at the flow rate of 2 mL min^{-1} : (a) 0.50×10^{-4}, (b) 1.00×10^{-4}, (c) 2.00×10^{-4}, (d) 3.00×10^{-4}, (e) 4.00×10^{-4}, (f) 5.00×10^{-4} M, for amino acids: (A) glycine, (B) threonine, (C) cysteine.

drift occurred presumably due to strong absorption of the thiol group at the electrode surface. This effect has also been observed when copper wire and copper tubular electrode were employed as potentiometric detector(96). Table 3.18 shows sensitivity of 86.66 $\mu A\ M^{-1}$ glycine, 108.34 $\mu A\ M^{-1}$ threonine and 199.20 $\mu A\ M^{-1}$ cysteine with respective correlation coefficient of 0.999, 0.999 and 0.998.

In any flow system the detection limit depends on a number of factors including the sensitivity of the sample, the noise level of the sample at low concentration and the extent of dispersion of the sample in the stream. The detection limit found here was 1.22×10^{-5} M glycine, 1.17×10^{-5} M threonine and 1.19×10^{-5} M cysteine. The summary of these results is shown in Table 3.18.

Table 3.15 Effect of glycine concentration on peak current in FIA in phosphate buffer pH 7.0 at the flow rate of 2 mL min^{-1}.

[glycine],M	peak current,μA
5.00×10^{-4}	0.03
2.00×10^{-3}	0.15
6.00×10^{-3}	0.48
1.00×10^{-2}	0.79
2.00×10^{-2}	1.69
4.00×10^{-2}	3.58
6.00×10^{-2}	5.10
8.00×10^{-2}	6.70
1.00×10^{-1}	8.73

Table 3.16 Effect of threonine concentration on peak current in FIA in phosphate buffer pH 7.0 at the flow rate of 2 mL min^{-1}.

[threonine],M	peak current,μA
5.00×10^{-4}	0.07
2.00×10^{-3}	0.27
6.00×10^{-3}	0.82
1.00×10^{-2}	1.31
2.00×10^{-2}	2.39
4.00×10^{-2}	4.58
6.00×10^{-2}	6.70
8.00×10^{-2}	8.88
1.00×10^{-1}	10.81

Table 3.17 Effect of cysteine concentration on peak current in FIA in phosphate buffer pH 7.0 at the flow rate of 2 mL min^{-1}.

[cysteine],M	peak current,μA
5.00×10^{-5}	0.008
1.00×10^{-4}	0.018
5.00×10^{-4}	0.086
1.00×10^{-3}	0.181
2.00×10^{-3}	0.418
4.00×10^{-3}	0.830
6.00×10^{-3}	1.167

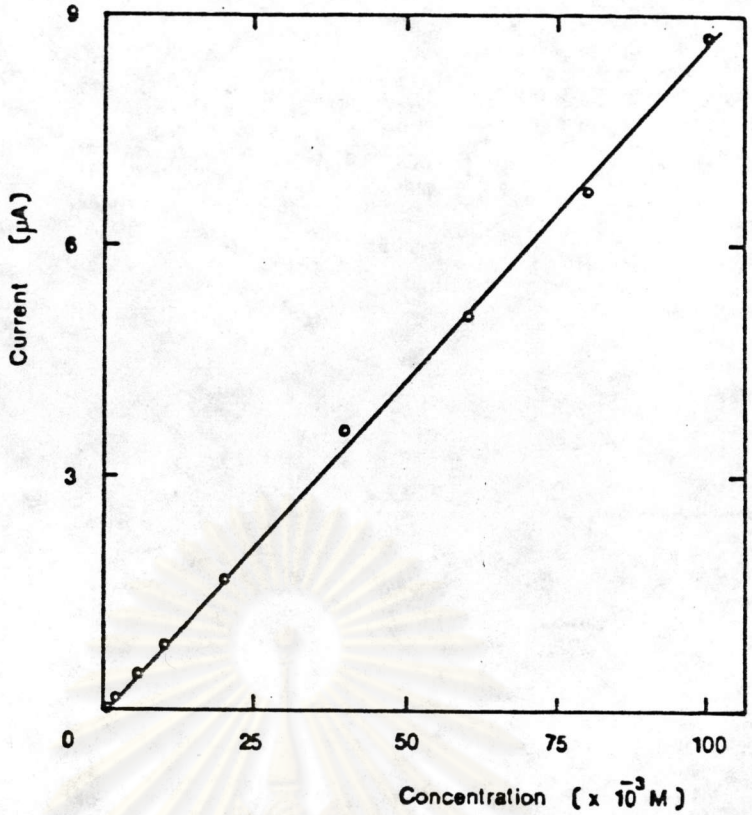

Figure 3.13 Calibration of glycine in the concentration range of 5.00×10^{-4} -1.00×10^{-1} M at a copper electrode with 10.0 μL injection, at the flow rate of 2 mL min^{-1}

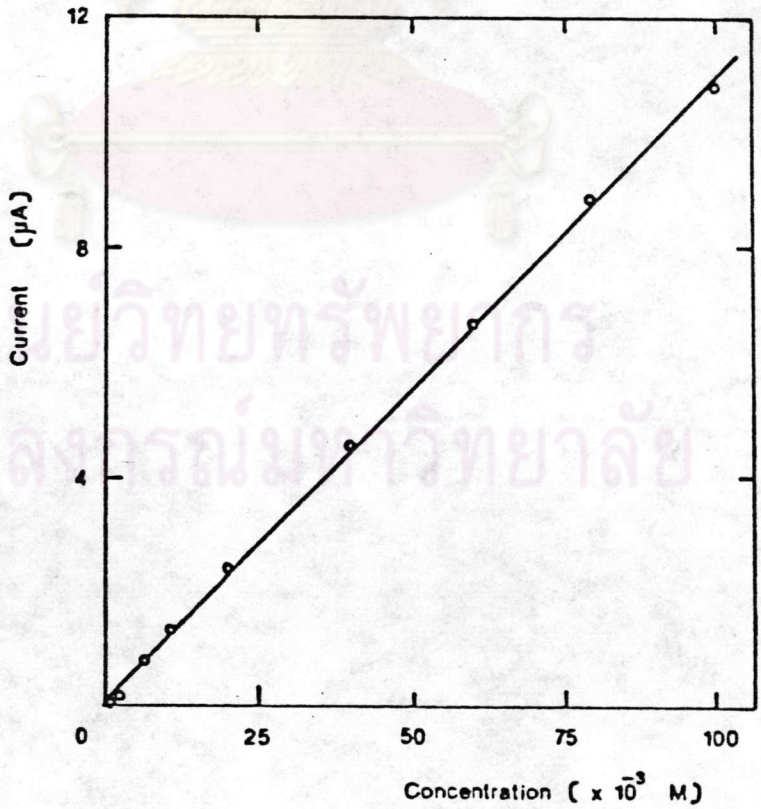

Figure 3.14 Calibration of threonine in the concentration range of 5.00×10^{-4} -1.00×10^{-1} at a copper electrode with 10.0 μL injection, at the flow rate of 2 mL min^{-1}.

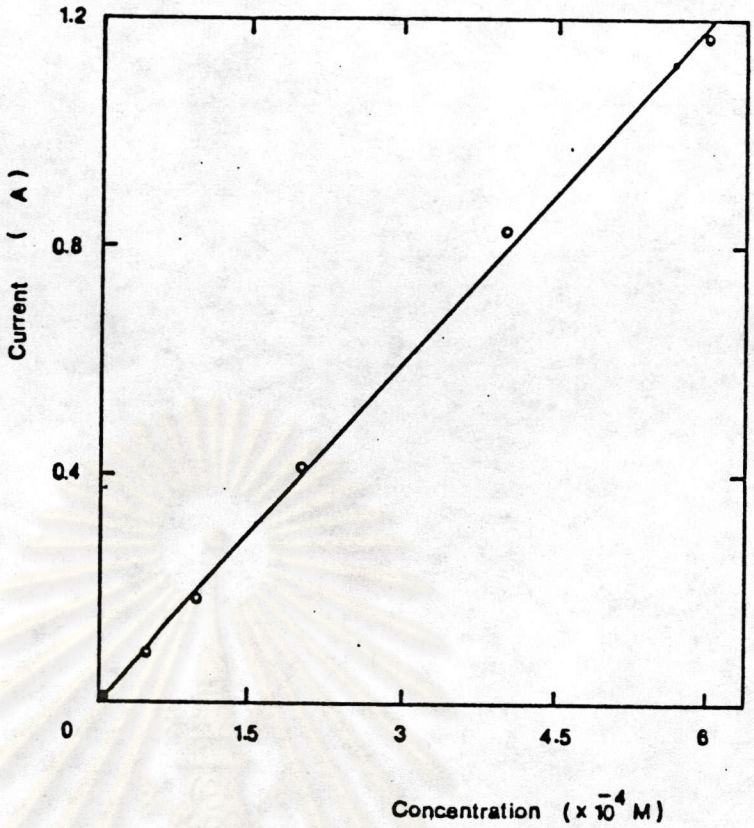

Figure 3.15 Calibration of cysteine in the concentration range of 5.00×10^{-5} -6.00×10^{-3} M at a copper electrode with 10.0 µL injection, at the flow rate of 2 mL min^{-1}.

Table 3.18 Hydrodynamic electrochemical characteristics at a copper electrode in phosphate buffer pH 7.0

amino acid	linear range M	sensitivity $\mu A\ M^{-1}$	detection limit M
glycine	5.00×10^{-4} -1.00×10^{-1}	86.66	1.22×10^{-5}
threonine	5.00×10^{-4} -1.00×10^{-1}	108.34	1.17×10^{-5}
cysteine	5.00×10^{-5} -6.00×10^{-3}	119.20	1.19×10^{-5}

3.2.5 Effect of Sample Injection Volume

Injections of a fixed concentration of glycine (0.01M) using aliquots of 2.0-8.0 µL gave peak heights linear with µg injected as shown in Figure 3.16 and the results are summarized in Table 3.19. Linear regression analysis of the calibration curve in Figure 3.17 gives a correlation coefficient of 0.999 and a slope of 105.26 nA μg^{-1} injected. This value of sensitivity is in agreement with the value of 115.15 nA μg^{-1} (86.66 $\mu A\ M^{-1}$) reported in 3.2.4. Therefore, in FIA the calibration curves can be made by either varying the concentration of sample injected or varying the volume of injected sample at fixed concentration.

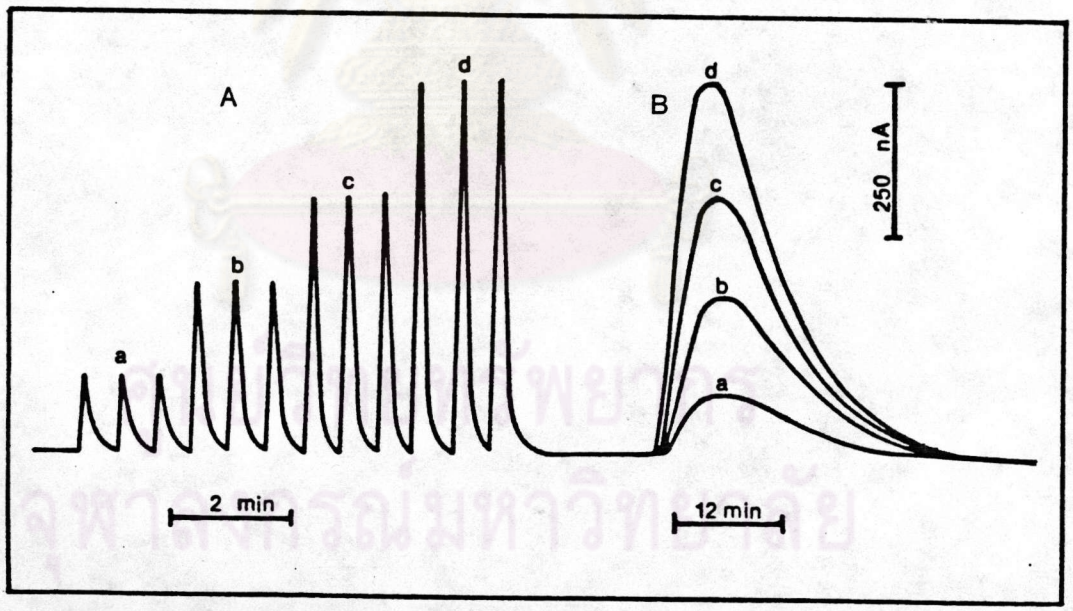

Figure 3.16 Effect of sample injection volume on sample peak at the flow rate of 2 mL min^{-1} : (a) 2.0, (b) 4.0, (c) 6.0, (d) 8.0 µL for glycine at 0.01 M, recorded at different chart speeds: (A) 10 ; (B) 100 mm min^{-1}

Table 3.19 Effect of sample injection volume on peak current of 0.01M glycine in phosphate buffer pH 7.0 at the flow rate of 2 mL min^{-1}.

injection volume µL	g injected $x10^{-3}$ M	peak current nA
2	1.5	136.70
4	3.0	286.70
6	4.5	438.30
8	6.0	615.00

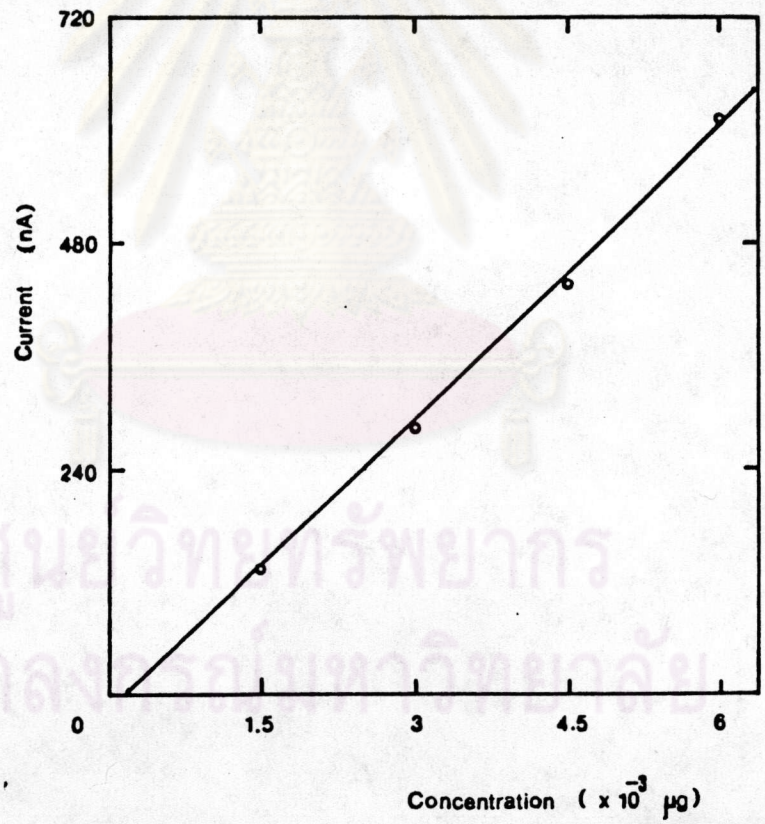

Figure 3.17 Calibration curve of glycine at the anodized copper electrode with 2-8 µL injection of 0.01 M glycine in phosphate buffer pH 7.0.

3.3 Application of a Copper Electrode as an Amperometric Detector in Amino Acids Analysis by HPLC

The effect of buffer system on the response of copper electrode was discussed in 3.1, wherein it was shown that the optimum system was phosphate buffer pH 7.0. Generally , in the analysis by HPLC the polarity of mobile phase must be varied to find the best mobile phase for the separation . The polarity of mobile phase in this study was varied by adding methanol (MeOH) to the phosphate buffer pH 7.0 in various ratios. The effect of mobile phase on retention time and peak current, sensitivity, linear range , reproducibility and detection limit of five amino acids, such as threonine, methionine, arginine, phenylalanine and tryptophan, are examined at the copper electrode in the reversed phase HPLC system.

3.3.1 Effect of Percentage of MeOH in Mobile Phase

Figure 3.18 shows chromatograms of the separation of five amino acids on an ODS column, with the mixed methanol-phosphate buffer pH 7.0 at various ratios as the mobile phase at the flow rate of 1 mL min^{-1} . The retention times and peak heights of these amino acids at each ratio of methanol in the mobile phase are summarized in Table 3.20. The results show that increasing the amount of methanol gave rise to progressive reduction in retention time, and subsequent losses in resolution and reduction in the peak current were due to the decrease in the conductivity of the mobile phase. The mobile phase of 10.0% methanol in phosphate buffer pH 7.0 was found to be the most suitable for the separation of these five amino acids according to the results of good separation, high peak current and short elution time.

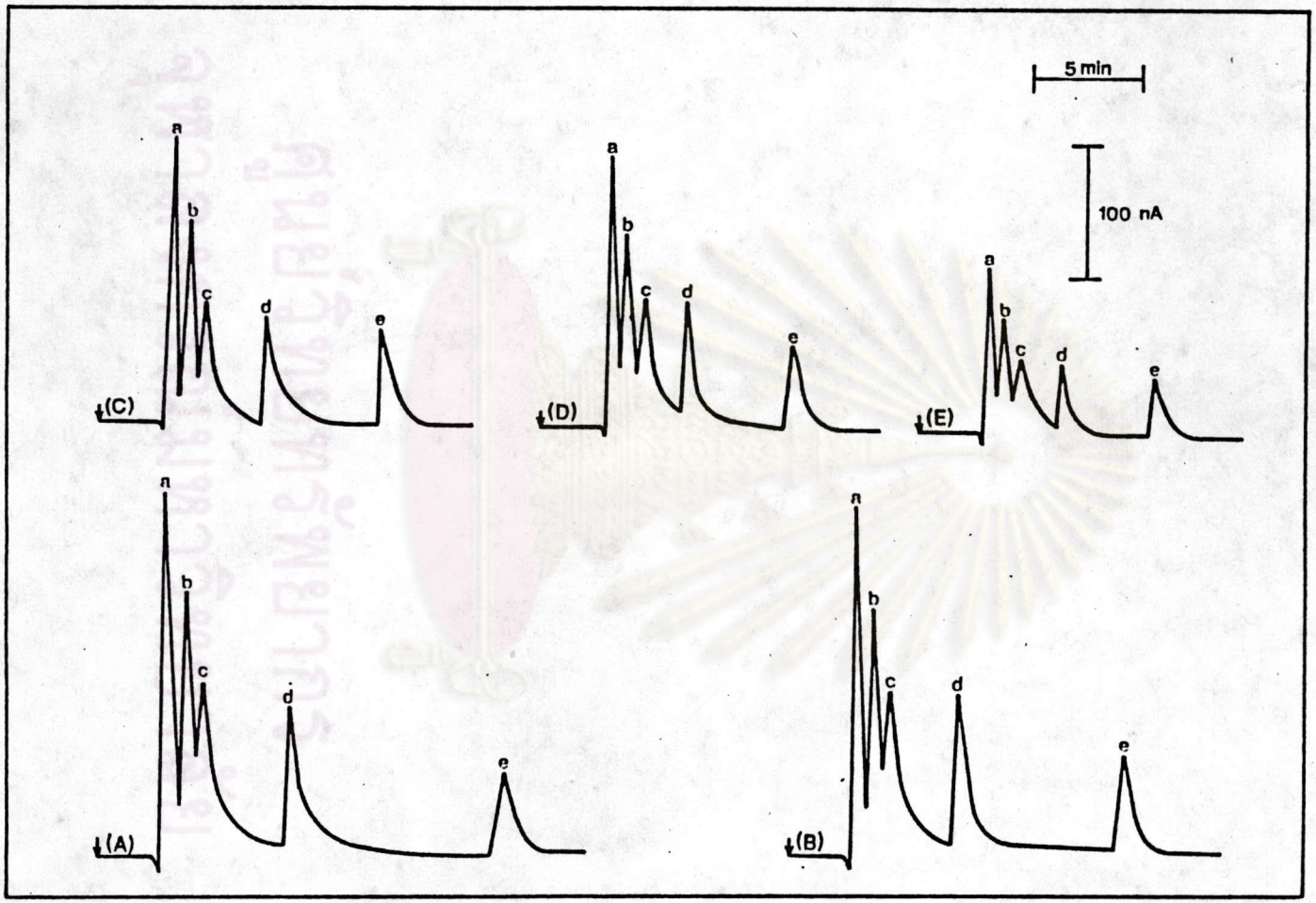

Figure 3.18 Chromatograms of the separation of five amino acids on ODS column, with the following mobile phase: (A) 2.5%, (B) 5.0%, (C) 7.5%, (D) 10.0%, (E) 15.0% MeOH in phosphate buffer pH 7.0, for amino acids: (a) threonine, (b) methionine, (c) arginine, (d) phenylalanine, (e) tryptophan at 1.60×10^{-3} M.

Table 3.20 Effect of percentage of methanol in the mobile phase on retention time and peak current of five amino acids at 1.60×10^{-3} M.

%MeOH	threonine		methionine		arginine		phenylalanine		tryptophan	
	t_R	i	t_R	i	t_R	i	t_R	i	t_R	i
2.5	3.09	269.00	4.12	162.00	4.82	77.00	8.65	111.00	18.23	63.00
5.0	3.09	231.00	3.97	137.00	4.70	62.00	7.59	102.00	14.82	66.00
7.5	3.06	198.00	3.74	107.00	4.59	60.00	6.53	86.00	11.29	68.00
10.0	3.11	187.00	3.79	104.00	4.59	58.00	6.41	87.00	10.70	71.00
15.0	3.11	132.00	3.68	58.00	4.59	44.00	5.62	.61.00	8.32	56.00

t_R = retention time in min

i = peak current in nA

3.3.2 Sensitivity and Linear Range

The linear dynamic range of the detector was determined for 20.0 µL amino acid samples. The effect of concentration of threonine ,methionine, arginine, phenylalanine and tryptophan on peak current and calibration plots are shown in Table 3.21 and Figure 3.19-3.23, respectively. The calibration plots of these amino acids are linear in the range of 10^{-4} -10^{-3} M. The slope of these calibration plots are 93.46 µA M^{-1} threonine, 73.63 µA M^{-1} methionine, 43.10 µA M^{-1} arginine ,43.67 µA M^{-1} phenylalanine and 36.63 µA M^{-1} tryptophan with respective correlation coefficient of 0.999, 0.999, 0.999, 0.999 and 0.998. The summary of these values is shown in Table 3.22.

Table 3.21 Effect of amino acid concentrations on the peak current in HPLC with 10.0% MeOH in phosphate buffer pH 7.0 as mobile phase at the flow rate of 1 mL min^{-1}.

amino acid	concentration $x10^{-4}$ M	peak current nA
threonine	2.00	20.80
	4.00	40.67
	6.00	61.67
	8.00	80.50
	10.00	100.70
	12.00	116.30
	14.00	132.50
	16.00	152.50
methionine	2.00	16.30
	4.00	34.00
	6.00	48.00
	8.00	63.67
	10.00	79.00
	12.00	91.33
	16.00	122.00
arginine	2.00	8.80
	4.00	17.67
	6.00	26.00
	8.00	35.67
	10.00	44.33
	12.00	52.00
	14.00	60.67
	16.00	69.00
	18.00	78.50
	20.00	86.50
phenylalanine	2.00	8.80
	4.00	18.00
	6.00	29.33
	8.00	35.33
	10.00	44.69
	12.00	52.33
tryptophan	2.00	8.70
	4.00	17.67
	6.00	24.67
	8.00	30.33
	10.00	39.33
	12.00	45.50
	14.00	53.67

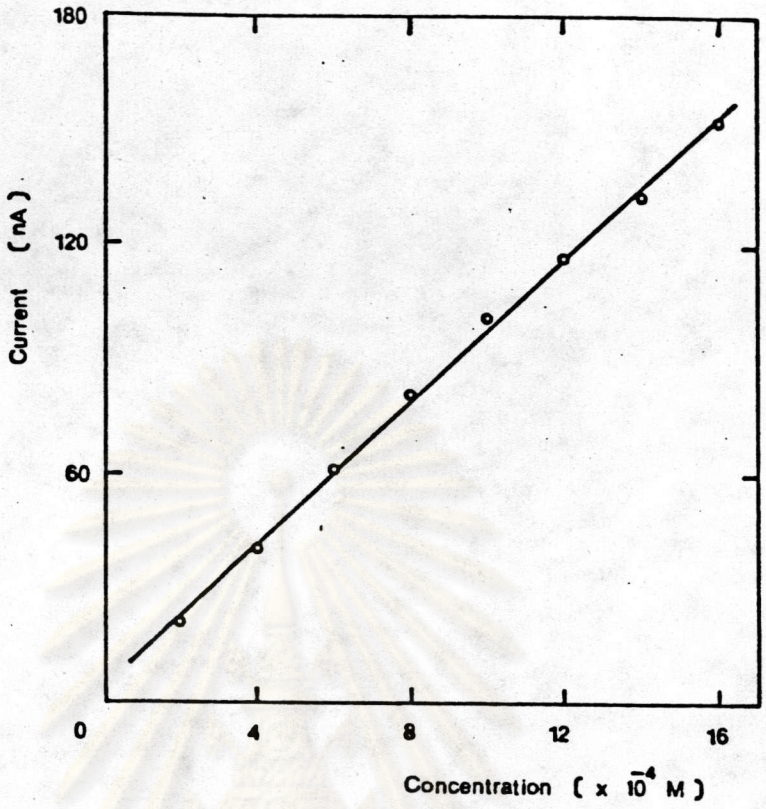

Figure 3.19 Calibration plot of threonine

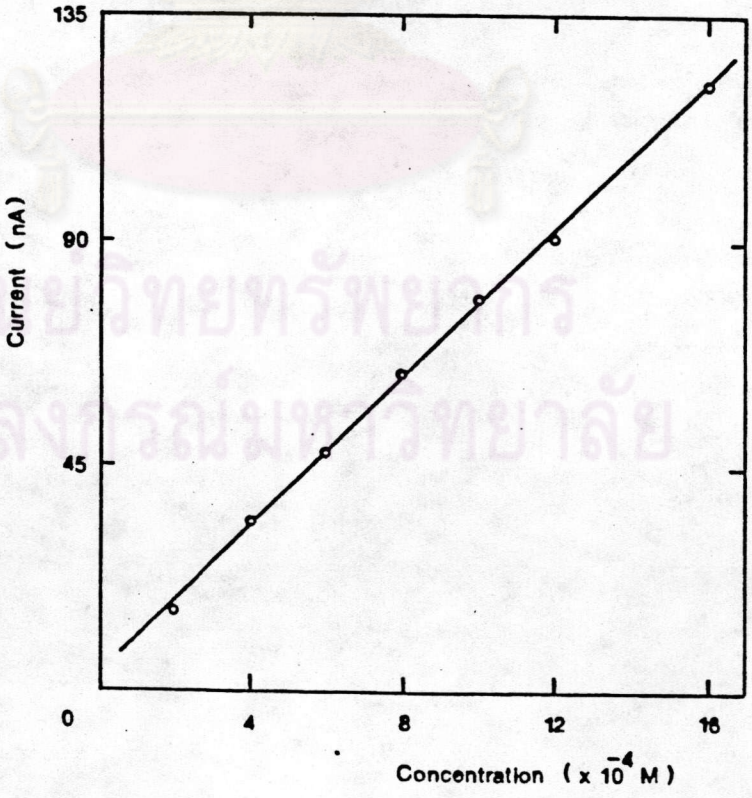

Figure 3.20 Calibration plot of methionine

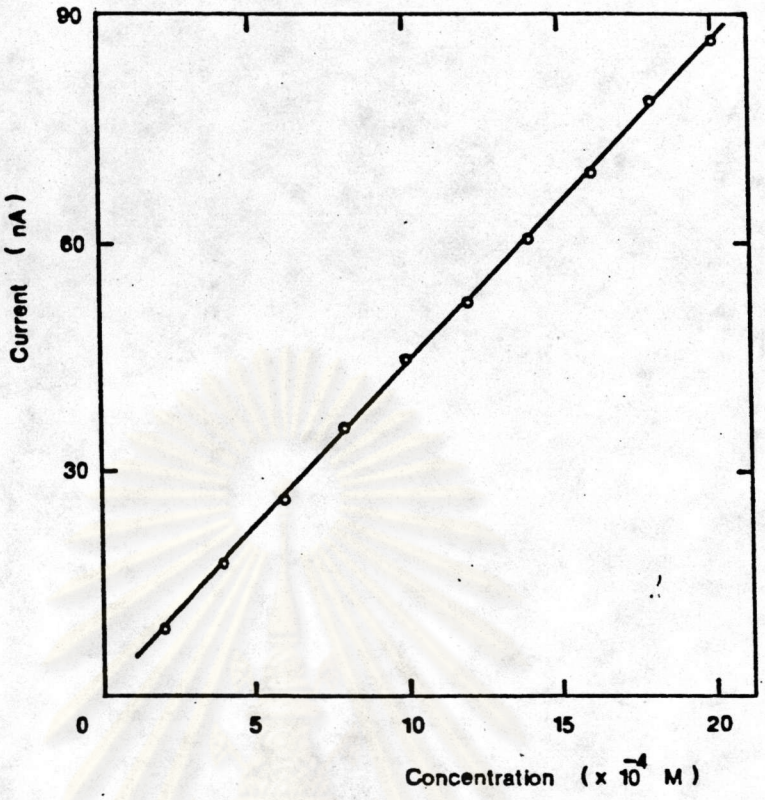

Figure 3.21 Calibration plot of arginine

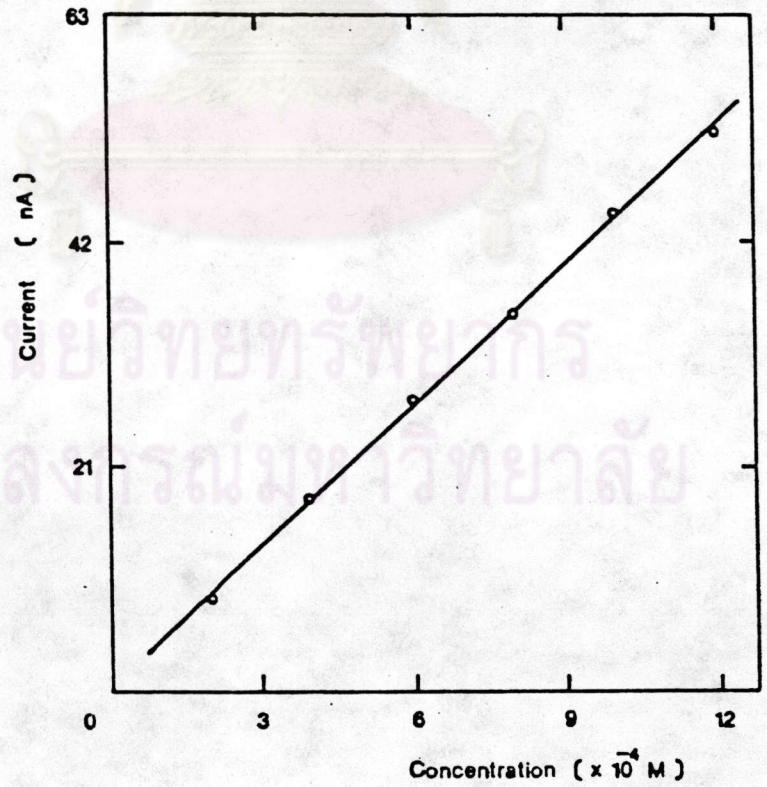

Figure 3.22 Calibration plot of phenylalanine

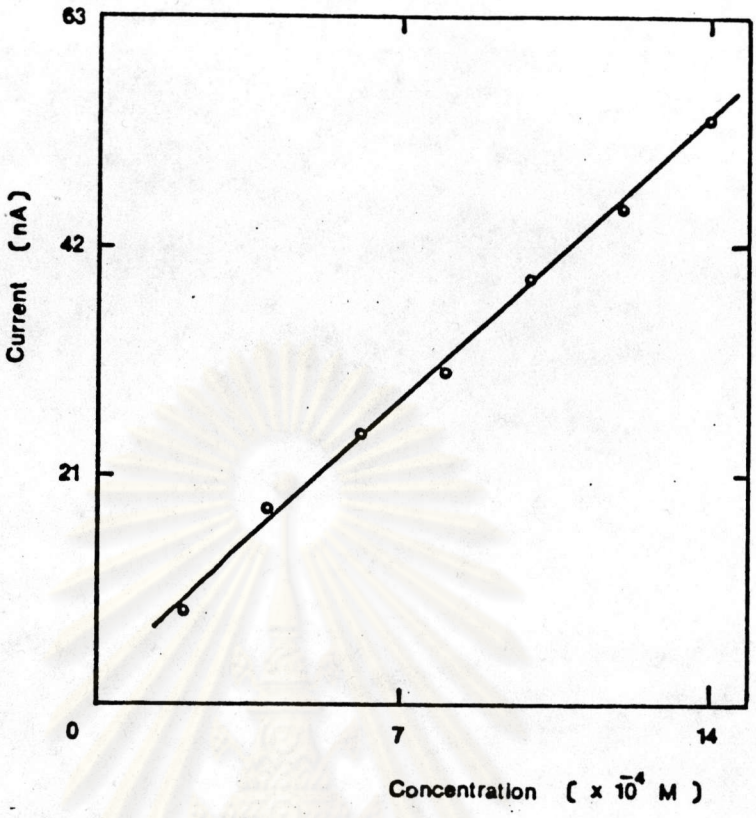

Figure 3.23 Calibration plot of tryptophan

Table 3.22 Electrode characteristics in HPLC with 10.0% MeOH in phosphate buffer pH 7.0 as mobile phase at the flow rate of 1 mL min^{-1}

amino acid	sensitivity $\mu A\ M^{-1}$	linear range M	detection limit M
threonine	93.46	2.00×10^{-4} - 1.60×10^{-3}	1.20×10^{-5}
methionine	73.63	2.00×10^{-4} - 1.60×10^{-3}	2.32×10^{-5}
arginine	43.10	2.00×10^{-4} - 2.00×10^{-3}	2.05×10^{-5}
phenylalanine	43.67	2.00×10^{-4} - 1.20×10^{-3}	1.80×10^{-5}
tryptophan	36.63	2.00×10^{-4} - 1.40×10^{-3}	1.60×10^{-5}

3.3.3 Reproducibility and Detection Limit

The detection limits of threonine, methionine, arginine, phenylalanine and tryptophan, taken as 3 SD of ten replicates of 1.00×10^{-4} M amino acid, were 1.20×10^{-5} M, 2.32×10^{-5} M, 2.05×10^{-5} M, 1.80×10^{-5} M and 1.60×10^{-5} M, respectively (Table 3.20). The reproducibility of 1.20×10^{-3} M of each amino acid was examined and the results were shown in Table 3.21 that, the relative standard deviations were 1.77% for threonine, 2.16% for methionine, 2.51% for arginine, 0.72% for phenylalanine and 1.49% for tryptophan.

Table 3.23 Reproducibility (%RSD) of 1.20×10^{-3} M amino acid.

n	peak current of 1.20×10^{-3} M amino acid , nA				
	threonine	methionine	arginine	phenylalanine	tryptophan
1	105.00	66.00	45.00	52.00	64.00
2	107.00	66.00	45.00	52.00	64.00
3	111.00	70.00	43.00	51.00	64.00
4	107.00	69.00	43.00	52.00	64.00
5	109.00	68.00	43.00	52.00	62.00
6	109.00	68.00	45.00	52.00	62.00
mean	108.00	67.83	44.00	51.83	63.33
%RSD	1.77	2.16	2.27	0.72	1.49